Catalysis Science & Technology

RSC Publishing

COMMUNICATION

View Article Online
View Journal | View Issue

Cite this: *Catal. Sci. Technol.*, 2013, **3**, 2555

Received 29th May 2013,
Accepted 5th July 2013

DOI: 10.1039/c3cy00372h

www.rsc.org/catalysis

Superior activity of rutile-supported ruthenium nanoparticles for HCl oxidation†

Evgenii V. Kondratenko,[a] Amol P. Amrute,[b] Marga-Martina Pohl,[a] Norbert Steinfeldt,[a] Cecilia Mondelli[b] and Javier Pérez-Ramírez*[b]

The activity of supported Ru-based catalysts in the oxidation of HCl to Cl_2 is shown to be strongly affected by active phase–support interactions and by the way of incorporation of the Ru species. Depositing colloidally prepared Ru nanoparticles on a rutile carrier results in catalysts attaining very high and stable HCl conversion levels under industrially-relevant conditions using ruthenium loadings as low as 0.16 wt%.

Catalysts featuring supported metals or metal oxides are applied in numerous commercial processes to convert abundant raw materials into higher-value products ranging from fuels to plastics, resins, and pharmaceuticals. Their performance is typically determined by the chemical or structural nature of the deposited species, their electronic and/or acid–base properties, and the active phase–support interactions.[1–5] Therefore, synthetic control over all these parameters is critical for designing optimised catalysts, from the viewpoints of performance and active phase utilisation. Recently, various routes have been developed to prepare metal nanoparticles (NPs) with well-defined size, shape, and chemical composition.[1,4,6,7] Noteworthily, the size of tailored NPs usually prepared in colloidal solutions[8,9] remains unaltered upon deposition onto typical catalyst carriers.[10,11] This enabled us to systematically investigate the effect of size and even shape of supported noble metal NPs on the activity and selectivity in both low-temperature hydrogenation[4,7,12] and high-temperature oxidation[10,11,13,14] reactions. Moreover, owing to the high metal utilisation and, thus, activity attained, it was possible to generate catalysts based on NPs with drastically reduced metal loadings, even down to 0.005 wt%, which still exhibited satisfactory performance.[11,14] Therefore, the use of NPs for developing novel catalysts is also attractive from economic and environmental perspectives.

The gas-phase oxidation of HCl to Cl_2 comprises a recent industrial process that would benefit from a decreased catalyst cost in order to achieve a wider application. This reaction represents a sustainable route to recycle by-product HCl streams in the phosgene-mediated manufacture of polyurethanes and polycarbonates.[15,16] $RuO_2/TiO_2/SiO_2$ and $RuO_2/SnO_2–Al_2O_3$ are the state-of-the-art catalysts, developed by Sumitomo and Bayer, respectively.[17–19] The choice of a support with identical structure (rutile type) and similar lattice parameters to the active phase has been indicated as one main reason for the outstanding performance of these materials, as maximum RuO_2 dispersion and stabilisation are expected through its epitaxial growth.[17] Due to the high and fluctuating market price of ruthenium (peak price at 600 USD per ounce in 2007),[15] considering a typical Ru loading of 1–2 wt%[18,20] leads to a metal cost associated to the catalyst for a world-scale HCl recycling facility (*ca.* 100 kton Cl_2 per year) of several million euros. Thus, catalysts containing a lower amount of ruthenium are highly desired but their activity and robustness should not be compromised. A first step in this direction is represented by the recent development by some of us of a $RuO_2/SnO_2–Al_2O_3$ system with 0.5 wt% Ru which displays excellent stability and an even double Ru-specific activity compared to the counterpart catalyst with 2 wt% Ru, likely due to an enhanced dispersion of the active phase.[18,19] As all these catalysts have been prepared by conventional impregnation of the carriers with a metal precursor solution, followed by calcination,[18–20] further catalyst optimisation might be achieved by variations in the synthetic strategy.

Herein, we show that the deposition of tailored Ru NPs on TiO_2-rutile with a metal loading as low as 0.16 wt% produces a highly active and stable material, while an identically prepared Al_2O_3-supported catalyst is virtually inactive. This result highlights the importance of the active phase–support interactions. Moreover, our novel rutile-based system exhibits a HCl conversion level close to that of a classically prepared reference RuO_2/TiO_2-rutile catalyst with a Ru loading in the range of those

[a] *Leibniz-Institut für Katalyse e.V. an der Universität Rostock, Albert-Einstein-Str. 29 A, D-18059 Rostock, Germany*

[b] *Institute for Chemical and Bioengineering, Department of Chemistry and Applied Biosciences, ETH Zurich, Wolfgang-Pauli-Strasse 10, CH-8093 Zurich, Switzerland. E-mail: jpr@chem.ethz.ch; Fax: +41 44 6331405; Tel: +41 44 6337120*

† Electronic supplementary information (ESI) available: Details of catalyst preparation, characterisation, and catalytic evaluation. Results from XPS of the as-prepared catalyst featuring Ru NPs on TiO_2-r and H_2-TPR of selected samples after use in HCl oxidation. See DOI: 10.1039/c3cy00372h

reported for the industrial systems (2 wt%).[18,20] The metal utilisation in this NP-based catalyst is significantly enhanced, as its Ru-related activity is 2 times higher than that of an impregnated catalyst with the same metal content (0.16 wt%) and 9 times higher than the reference catalyst. Its exceptional performance is explained by the extraordinarily high dispersion of the catalytically active RuO_2 species and by electronic effects of the TiO_2-rutile support. The former is demonstrated to originate from the reaction-induced oxidation of the initially metallic spherical Ru NPs and restructuring into thin plate-like RuO_2 structures, owing to the lattice matching with the support. The latter is shown to determine the generation of RuO_2 species featuring highly labile oxygen atoms.

The Ru NPs were prepared by the ethylene glycol (EG) method[21] and deposited on TiO_2-rutile (r), TiO_2-anatase (a), or γ-Al_2O_3 carriers with a metal loading of 0.16–0.4 wt%. For benchmarking purposes, we applied the dry impregnation (I) method to produce TiO_2-r-supported catalysts with 0.16 (RuO_2/TiO_2-I) and 2 wt% Ru (RuO_2/TiO_2-I-ref). Further details on these synthetic procedures are provided in the ESI.† Table 1 shows the actual metal loading and surface area of the catalysts. The double Ru content of the alumina-supported catalyst compared to the other catalysts attained using the EG route is likely due to the much larger surface area of this support.

The size and distribution of the Ru NPs in the synthesis solution were determined by small angle X-ray scattering (SAXS) in combination with the indirect Fourier transformation (IFT) technique. The resulting function of volume-weighted particle radius distribution is relatively narrow with a maximum at *ca.* 0.5 nm (Fig. S1 in the ESI†). Since the same colloidal solution was used for preparing the supported catalysts, the size of the Ru NPs deposited on the carriers was not expected to differ. The distribution and morphology of the supported ruthenium phase was analysed using high-angle annular dark field scanning transmission electron microscopy (HAADF-STEM). Accordingly, the Ru nanostructures appear bright in contrast to the background, which was confirmed by elemental energy-dispersive X-ray (EDX) analysis of selected regions of the images. Very small and well-distributed spherical NPs were obtained *via* the EG route on all of the carriers, as exemplified by the micrograph of the fresh Ru/TiO_2-r-EG catalyst (Fig. 1a). In line with the SAXS measurements, the size distribution of the supported species is also narrow (Fig. 1b). Their average diameter was estimated to be *ca.* 1.2 ± 0.25 nm. The originally metallic state of the NPs was maintained upon deposition on the support, as confirmed using X-ray photoelectron spectroscopy (XPS, Fig. S2, ESI†). As expected, the conventional impregnation method resulted in the formation of bigger (2–3 nm) nanostructures for the same metal loading (Fig. 1c). In this case, their nature is oxidic due to the calcination step.

Table 1 Characterisation and catalytic data of supported RuO_2 catalysts

Catalyst	Ru[a] (wt%)	S_{BET}[b] (m^2 g^{-1})	X_{HCl}[c] (%)	r[c] (mol Cl_2 min^{-1} mol Ru^{-1})
RuO_2/TiO_2-r-EG	0.16	29 (28)[d]	51	48
RuO_2/TiO_2-a-EG	0.17	54 (51)	22	19
RuO_2/γ-Al_2O_3-EG	0.40	149 (156)	4	1.4
RuO_2/TiO_2-r-I	0.16	33 (26)	23	21
RuO_2/TiO_2-r-I-ref	2.00	30 (29)	70	5.3

[a] Determined by ICP-OES. [b] N_2 sorption at 77 K. [c] Conditions: W = 0.25 g, T_{bed} = 623 K, O_2/HCl = 2, F_T = 166 cm^3 STP min^{-1}, t = 2 h, and P = 1 bar. [d] Surface area of the samples after Deacon reaction in parentheses.

To elucidate the effect of the carrier nature and of the preparation method on the activity of the supported Ru NP-containing catalysts in the gas-phase oxidation of HCl to Cl_2, catalytic tests were performed in a continuous-flow micro-reactor (details are provided in the ESI†). In view of the presence of excess O_2 in the reaction mixture, we questioned whether the metallic Ru NPs underwent oxidation upon use. To clarify this point, selected catalysts applied for 2 h in the reaction were characterised by temperature-programmed reduction with hydrogen (H_2-TPR). Hydrogen consumption below 550 K was observed (Fig. S3, ESI†), which corresponds to the reduction of RuO_2 to Ru,[22] thus indicating the *in situ* formation of an oxidic phase. This implies, from a kinetic viewpoint, that the rate of interaction of gaseous O_2 with metallic Ru is significantly higher than the rate of removal of adsorbed oxygen species by HCl. Thus, irrespective of the method of catalyst preparation, RuO_2 species are active for the oxidation of HCl to Cl_2. This justifies the usage of RuO_2 instead of Ru in the catalysts' nomenclature.

The HCl conversion was strongly affected by both the structure of the supporting oxide and the synthetic procedure (Table 1). With regard to the first aspect, among the catalysts prepared *via* the colloidal route, RuO_2/TiO_2-r-EG showed the highest HCl conversion, which was approximately 2 and 13 times higher than for RuO_2/TiO_2-a-EG and RuO_2/γ-Al_2O_3-EG, respectively. This activity order resembles the previously reported relative activity of classically prepared catalysts featuring supported RuO_2 species.[17] Thus, the role of the carrier is decisive regardless of the method of preparation and deposition of the catalytically active species. On the other hand, the activity of the TiO_2-r-supported catalysts is remarkably influenced by the way of incorporation of the Ru-containing phase. In fact, RuO_2/TiO_2-r-EG displayed more than double HCl conversion compared to the corresponding impregnated catalyst with identical metal loading (Table 1). Actually, the difference in activity would be even greater bearing in mind that (i) the catalytic tests were performed in an integral reactor and (ii) the negative effect of Cl_2 and H_2O on the HCl conversion (product inhibition) increases with the conversion. It must be highlighted that the RuO_2/TiO_2-r-EG catalyst exhibited only a slightly lower HCl conversion, but a Ru-specific rate of one order of magnitude higher, than the reference catalyst with a Ru loading of 2 wt% (RuO_2/TiO_2-r-I-ref, Table 1).[18]

In order to obtain kinetic insights into the superior performance of the novel NPs-based catalyst, we investigated the effects of temperature and O_2/HCl ratio on its activity. Interestingly, the apparent activation energy and reaction order in O_2 for RuO_2/TiO_2-r-EG (66 kJ mol^{-1} and 0.5) were very similar to those for RuO_2/TiO_2-r-I (64 kJ mol^{-1} and 0.5) (Fig. 2a and b). These results indicate that the deposition method of the RuO_2 species does not alter the representative kinetic fingerprints of HCl oxidation. Furthermore, the stable HCl conversion of RuO_2/TiO_2-r-EG during a 50 h catalytic run (Fig. 2c) demonstrated that

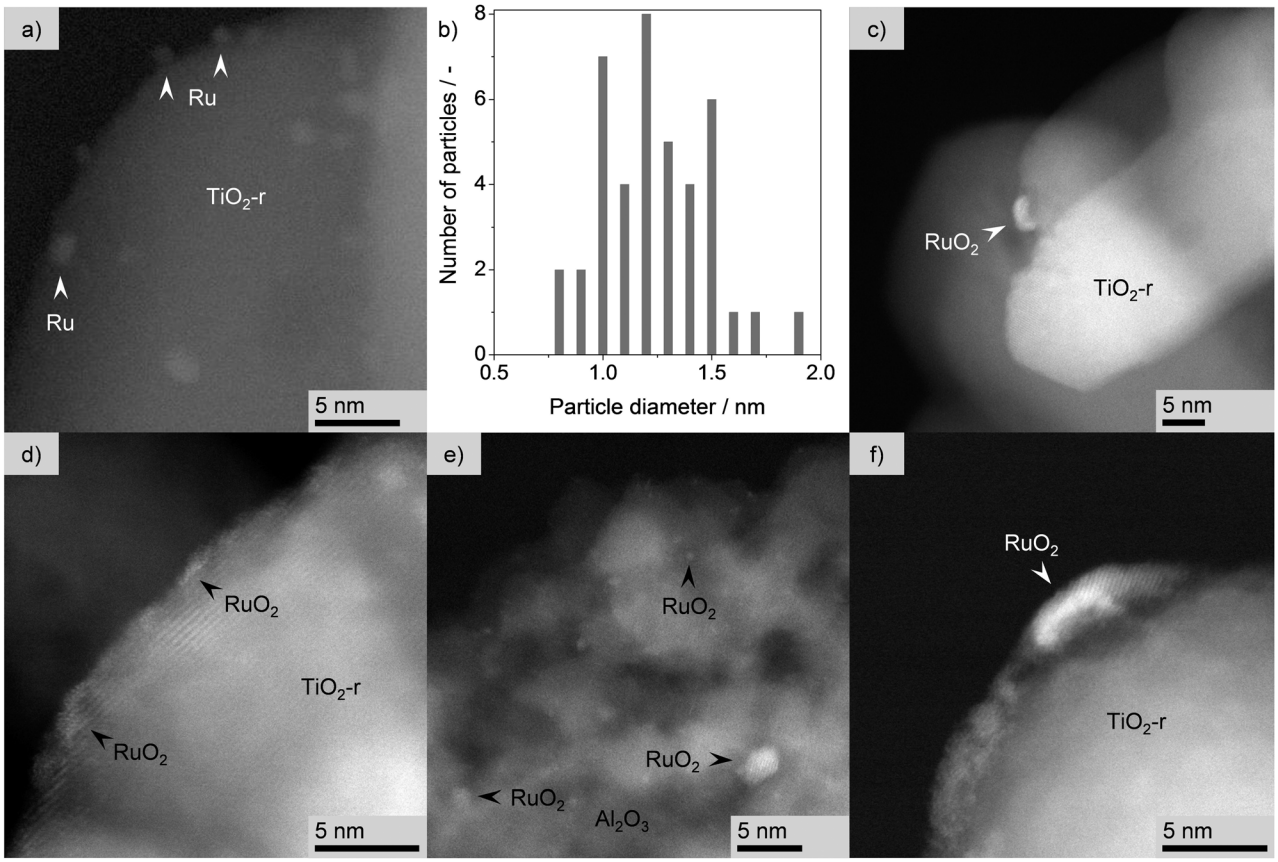

Fig. 1 HAADF-STEM of RuO_2/TiO_2-r-EG (a and d), RuO_2/TiO_2-r-I (c and f), and RuO_2/Al_2O_3-EG (e) in fresh form (a and c) and after HCl oxidation (d–f). Size distribution of the supported particles in fresh RuO_2/TiO_2-r-EG (b).

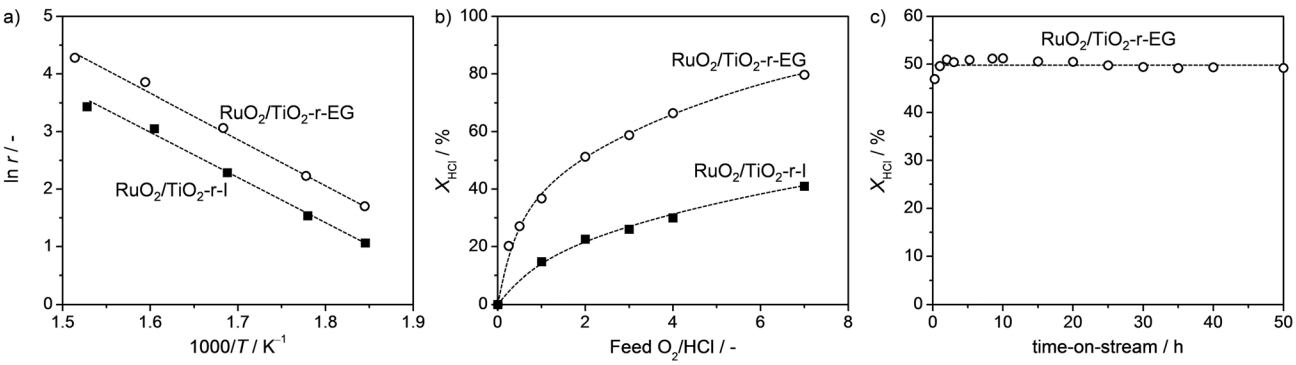

Fig. 2 Comparative performance of RuO_2 (0.16 wt% Ru)/TiO_2-r prepared by the ethylene glycol route (EG) and by dry impregnation (I): Arrhenius plot at T_{bed} = 543–653 K and O_2/HCl = 2 (a), dependence of the HCl conversion on the feed O_2/HCl ratio at T_{bed} = 623 K (b), and long catalytic run at T_{bed} = 623 K and O_2/HCl = 2 (c). Other conditions: W = 0.25 g, F_T = 166 cm^3 STP min^{-1}, and P = 1 bar. Data were acquired after 1 h under each condition for (a) and (b).

this synthetic procedure also leads to a catalyst with potential technical relevance.

In order to rationalise the support effect, since all systems studied feature RuO_2 species, we first explored whether their distinctive performance could be related to differences in morphology of the active phase. Based on the HAADF-STEM images of the used samples (Fig. 1d–f), it appears that the initially spherical Ru NPs on Al_2O_3 did not change their original form, while those on TiO_2-r were partially transformed into plate-like RuO_2 structures. The restructuring of the Ru NPs on TiO_2-r is explained on the basis of the matching between TiO_2-r and RuO_2 in terms of lattice symmetry and parameters (see scheme in the graphical abstract). The structural analogy of carrier and active phase has been already shown to drive the deposition of RuO_2 as an epitaxial layer over the carrier in classically prepared catalysts with higher Ru loading.[17,22]

This effect is further supported by the identification of plate-like RuO_2 structures also on the surface of RuO_2(0.16 wt% Ru)/TiO_2-r-I (Fig. 1d). Although a statistically relevant quantitative determination of the thickness of the RuO_2 platelets in RuO_2/TiO_2-r-EG is challenging, the thickness and size of the RuO_2 layers formed *via* impregnation appeared significantly larger than those attained from the well-defined Ru NPs. This is probably due to the fact that the latter species transform easier into thin RuO_2 layers than larger aggregates already in oxidic form.

The described morphology change of the TiO_2-r-supported Ru NPs is expected to determine a somewhat higher Ru dispersion for RuO_2/TiO_2-r-EG than for the other catalysts obtained *via* the EG route. Possibly, a larger fraction of the intrinsically more active and stable RuO_2 (110) facet is also exhibited in the platelets in line with the higher exothermic adhesion energy on TiO_2-r calculated for this compared to other exhibited RuO_2 surfaces.[22,23] Nevertheless, the TiO_2-r support should exert additional promoting effect(s) to account for the much higher HCl oxidation activity of RuO_2/TiO_2-r-EG. Based on the H_2-TPR analysis of the used catalysts, we put forward the existence of electronic interactions. The reduction profile of RuO_2-/TiO_2-r-EG (Fig. S3, ESI†) in fact evidences an additional H_2 consumption peak with a maximum at 368 K, which suggests the presence of RuO_2 species featuring labile lattice oxygen species. The great relevance of these species for the catalytic activity certainly deserves a precise elucidation of their nature and impact on the HCl oxidation at a molecular level. However, this would require the application of advanced characterization techniques and probably the support of theoretical calculations, which is out of the scope of this paper. Still, it is worth mentioning that, as such a pronounced increase in Ru-specific activity is obtained only through the application of the EG synthesis route and for very low Ru loadings, the electronic effect of TiO_2-r might be amplified if the RuO_2 nanostructures are very small, thin, and highly dispersed. Nonetheless, considering that the activity of RuO_2/TiO_2-a-EG is much higher than that of RuO_2/γ-Al_2O_3-EG, we hypothesise that geometric and electronic effects may be relevant, although to a lesser extent, also for supports featuring different structures with respect to RuO_2, which should also be further investigated.

In summary, we have introduced an approach to prepare very active catalysts with extremely low Ru loading for the oxidation of HCl to Cl_2, which consists in the preparation of well-defined Ru nanoparticles in solution and their subsequent deposition on carriers. However, the support influences how the Ru NPs are transformed into catalytically active RuO_2 species in the course of the reaction. Owing to structural similarities between TiO_2-rutile and RuO_2, this support enables the transformation of initially spherical Ru NPs into thin plate-like RuO_2 structures resulting in an enhanced dispersion of the oxide species. Furthermore, it modifies the electronic properties of the supported RuO_2 phase, generating highly active species with labile oxygen atoms. The advantage of our approach has been demonstrated by the fact that the RuO_2 (0.16 wt% Ru)/TiO_2-r-EG catalyst shows similar HCl conversion to a classically prepared catalyst with a Ru loading in the range reported for industrial systems, *i.e.* about 13 times higher. Furthermore, this material displays appreciable long-term stability. In view of a potential practical application, it is also relevant to note that, although the synthetic approach utilised here to prepare and deposit Ru nanoparticles on carriers is not as standard in industrial practice as the classical impregnation methods, the procedure is amenable to large-scale production.

We thank Bayer MaterialScience AG for permission to publish these results.

Notes and references

1 J. M. Campelo, D. Luna, R. Luque, J. M. Marinas and A. A. Romero, *ChemSusChem*, 2009, **2**, 18.
2 F. Cavani, N. Ballarini and A. Cericola, *Catal. Today*, 2007, **127**, 13.
3 J. Macht and E. Iglesia, *Phys. Chem. Chem. Phys.*, 2008, **10**, 5331.
4 G. A. Somorjai and J. Y. Park, *Angew. Chem., Int. Ed.*, 2008, **47**, 9212.
5 S. L. Wegener, T. J. Marks and P. C. Stair, *Acc. Chem. Res.*, 2012, **45**, 206.
6 H. Cong and J. A. Porco, *ACS Catal.*, 2012, **2**, 65.
7 K. An and G. A. Somorjai, *ChemCatChem*, 2012, **4**, 1512.
8 I. Lee, F. Delbecq, R. Morales, M. A. Albiter and F. Zaera, *Nat. Mater.*, 2009, **8**, 132.
9 C.-K. Tsung, J. N. Kuhn, W. Huang, C. Aliaga, L.-I. Hung, G. A. Somorjai and P. Yang, *J. Am. Chem. Soc.*, 2009, **131**, 5816.
10 P. J. S. Prieto, A. P. Ferreira, P. S. Haddad, D. Zanchet and J. M. C. Bueno, *J. Catal.*, 2010, **276**, 351.
11 C. Berger-Karin, M. Sebek, M. Pohl, U. Bentrup, V. A. Kondratenko, N. Steinfeldt and E. V. Kondratenko, *ChemCatChem*, 2012, **4**, 1368.
12 S. Alayoglu, C. Aliaga, C. Sprung and G. A. Somorjai, *Catal. Lett.*, 2011, **141**, 914.
13 N. Perkas, Z. Zhong, L. Chen, M. Besson and A. Gedanken, *Catal. Lett.*, 2005, **103**, 9.
14 J. Schäffer, V. A. Kondratenko, N. Steinfeldt, M. Sebek and E. V. Kondratenko, *J. Catal.*, 2013, **301**, 210.
15 J. Pérez-Ramírez, C. Mondelli, T. Schmidt, O. F.-K. Schlüter, A. Wolf, L. Mleczko and T. Dreier, *Energy Environ. Sci.*, 2011, **4**, 4786.
16 H. Over, *Chem. Rev.*, 2012, **112**, 3356.
17 K. Seki, *Catal. Surv. Asia*, 2010, **14**, 168.
18 C. Mondelli, A. P. Amrute, F. Krumeich, T. Schmidt and J. Pérez-Ramírez, *ChemCatChem*, 2011, **3**, 657.
19 A. P. Amrute, C. Mondelli, T. Schmidt, R. Hauert and J. Pérez-Ramírez, *ChemCatChem*, 2013, **5**, 748.
20 K. Seki, *US2010/0068126*, 2010.
21 Y. Wang, J. Ren, K. Deng, L. Gui and Y. Tang, *Chem. Mater.*, 2000, **12**, 1622.
22 D. Teschner, R. Farra, L. Yao, R. Schloegl, H. Soerijanto, R. Schomaecker, T. Schmidt, L. Szentmiklosi, A. P. Amrute, C. Mondelli, J. Pérez-Ramírez, G. Novell-Leruth and N. Lopez, *J. Catal.*, 2012, **285**, 273.
23 G. Novell-Leruth, G. Carchini and N. López, *J. Chem. Phys.*, 2013, **138**, 194706.

